# Manipulating Deformable Linear Objects: Attachable Adjustment-Motions for Vibration Reduction

**Shigang Yue,* Dominik Henrich**
*Embedded Systems and Robotics (RESY)*
*Informatics Faculty*
*University of Kaiserslautern*
*67653 Kaiserslautern, Germany*
*e-mail: [shigang, henrich]@informatik.uni-kl.de;*
*http: // resy.informatik.uni-kl.de /*

Received 26 October 2000; accepted 9 February 2001

This paper addresses the problem of handling deformable linear objects in a suitable way to avoid acute vibration. Different types of adjustment-motions that eliminate vibration of deformable objects and that can be attached to the end of an arbitrary end-effector's trajectory are presented. For describing the dynamics of deformable linear objects, the finite element method is used to derive the dynamic differential equations. A genetic algorithm is used to find the optimal adjustment motion for each simulation example. Experiments are conducted to verify the presented manipulating method. 

## 1. INTRODUCTION

The automated handling and assembly of materials have been studied by many researchers in the areas of manufacturing, robotics, and artificial intelligence. Until now, most studies assume that the objects to be manipulated are rigid. However, deformable materials such as cables, wires, ropes, cloths, rubber tubes, sheet metals, paper sheets, and leather products can be found almost everywhere in the real world of industry and human life. In most cases, deformable materials and parts are still handled and assembled by humans. Practical methods for the automatic handling and manipulation of deformable objects are urgently required.

Previous research work involving the modeling and controlling of deformable linear objects (DLOs) such as beams, cables, wires, and tubes, etc., has been found, for example, in refs. 1–13. There are two basic methods for handling DLOs: one is the force-based method with a physical model[1,4,5,8,10,12]; the other is the vision-based modeless method.[2,7] Some researchers are trying to use hybrid methods

*Yue is a research fellow of the Alexander von Humboldt Foundation from Beijing Polytechnic University.

(i.e., force and vision sensors or other sensors) to cope with linear deformable materials.[3,6] On the other hand, Zheng et al.[13] derived strategies to insert a flexible beam into a hole without sensors, while Hirai et al.[9,11] presented a human skillful transplantation method. However, the above methods are specialized and confined to limited applications.

When a robot executes a manipulation task, its motion can be divided into several motion primitives, each of which has a particular target state to be achieved in the task context. These primitives are called ''skills.'' An adequately defined skill can have generality to be applied to various similar tasks. Until now, most of the research work on skill-based manipulation deals with rigid objects.[14,15]

Skill-based manipulation for handling deformable linear materials has been touched upon recently. For example, Henrich et al.[16] analyzed the contact states and point contacts of DLOs with regard to manipulation skills, Abegg et al.[17] studied the contact state transitions based on force and vision sensors and Remde et al.[18] discussed the problem of picking up DLOs by experimentation.

However, the effects of dynamic vibration were not taken into account in the skill-related work described above. The dynamic effects of deformable objects cannot be neglected, especially when the objects are moved quickly by a robot arm. As shown in Fig. 1, the uncertainty resulting from oscillation may cause failure in the insert-into-hole operation. Therefore, the vibration caused by inertia should be depressed during the motion or eliminated as soon as possible after the motion.

Vibration reduction of flexible structures has been a topic for many researchers, and the previous works were reviewed by Chen and Zheng.[19] They also presented a passive approach based on an open-loop concept for vibration-free handling of deformable beams; similar ideas can be found in refs. 20 and 21; which deal only with rigid bodies. However, application of the method presented by ref. 19 is limited due to its stable start condition and a relatively simple trajectory. In considering the complex manipulations involved in practical situations, such as avoiding obstacles, picking up, and insert-into-hole, the stable start condition cannot be satisfied easily.

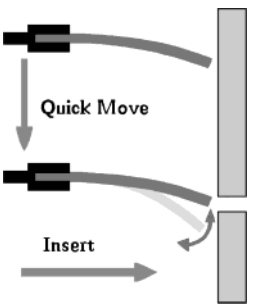


**Figure 1.** The quick operation causes uncertainty and failure.

In this article, we present attachable adjustment-motion at the end of an arbitrary trajectory of the end-effector. This attachable adjustment-motion can be treated as one of the vibration-free manipulation skills. Vibration caused during the arbitrary previous trajectory can be reduced during the attached adjustment-motion. Our approach also uses an open-loop concept. The suitable adjustment motion can be found by applying optimization methods. Additionally, the adjustment-motion is chosen to be as simple as possible, so that it may be easily utilized.

The rest of this paper consists of five parts. First, a finite element model for describing the dynamics of deformable linear objects is presented, wherein gravity is also taken into account. Second, the adjustment-motion is specified. Third, a method that uses genetic algorithms for generating the adjustment-motion is given. Then, several cases based on the model and method are presented. Finally, an experiment is conducted to verify the manipulating method.

## 2. DYNAMIC MODELING OF DLOs

The dynamic behavior of DLOs varies and depends upon the type of material involved; for example, cables are different from rubber bars. Furthermore, the behavior also depends on the length of the DLOs.[16] Finite element methods will be used in this paper to describe the dynamics of deformable linear objects. Only the elastic deformation of DLOs is considered; plastic deformation will be disregarded.

Figure 2 shows a generalized deformable element used here with eight parameters. The transverse deflections of the element are modeled by a quintic polynomial and the longitudinal deflections are assumed to be a linear polynomial.[22,23] The coordinates of the element are assembled in a vector

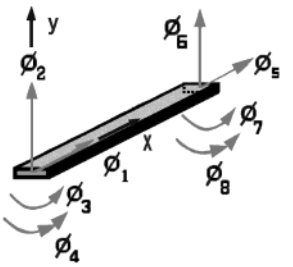


**Figure 2.** Parameters of a generalized element.

form as

$$\vec{\phi}_e = (\phi_1 \;\; \phi_2 \;\; \cdots \;\; \phi_8)^T \tag{1}$$

where $\phi_1$ and $\phi_5$ are the axial displacements along the $x$ axis, $\phi_2$ and $\phi_6$ are the transverse displacements along the $y$ axis, $\phi_3$ and $\phi_7$ are the rotary displacements about the $z$ axis, and $\phi_4$ and $\phi_8$ are the curvature displacements in the $xy$ plane.

The longitudinal deformation $D_{xe}$ and the transverse deformation $D_{ye}$ at an arbitrary point $p$ on the axis of an element can be expressed as follows,

$$D_{xe} = \vec{\phi}_e^T \vec{D}_x \tag{2}$$

$$D_{ye} = \vec{\phi}_e^T \vec{D}_y \tag{3}$$

where $\vec{D}_x$ and $\vec{D}_y$ are the vectors of the interpolation polynomials and can be found in the Appendix.

Before the dynamic equation can be obtained, it is necessary to derive the kinetic and potential energy of the element.

The velocity at point $p$ is given by

$$\vec{V}_p = \begin{bmatrix} \vec{i} & \vec{j} \end{bmatrix} \begin{bmatrix} V_{ax} - \dot{q} D_{ye} + \dot{D}_{xe} \\ V_{ay} + \dot{q}(x + D_{xe}) + \dot{D}_{ye} \end{bmatrix} \tag{4}$$

where $\vec{i}$ and $\vec{j}$ are the unit vectors of the floating coordinate system with $x$ and $y$ as axis and point $a$ as origin, and $V_{ax}$ and $V_{ay}$ are the projections of velocity at point $a$ on the $x$ and $y$ axis, respectively.

The kinetic energy of a DLO element can be expressed as

$$T = \frac{1}{2} \int_0^L \lambda \vec{V}_p^2 \, dx \tag{5}$$

where $\lambda$ is the mass of unit length, and $L$ is the length of the element. Substitution of Eqs. (2) and (3) into Eq. (4) and then substitution of Eq. (4) into Eq. (5) with subsequent rearrangement yields

$$\begin{aligned} T = {} & \frac{1}{2}\lambda \left( V_{ax}^2 L + V_{ay}^2 L + \frac{1}{3}\dot{q}^2 L^3 + V_{ay}\dot{q} L^2 \right) + \frac{1}{2}\lambda \dot{q}^2 \frac{IL}{A} \\ & + \frac{1}{2}\dot{q}^2 \vec{\phi}_e^T [m] \vec{\phi}_e + \frac{1}{2}\dot{\vec{\phi}}_e^T [m^+] \dot{\vec{\phi}}_e + \dot{q} \dot{\vec{\phi}}_e^T [B] \vec{\phi}_e \\ & + \vec{\phi}_e^T \{y^+\} + \dot{\vec{\phi}}_e^T \{x^+\} + \dot{q} \dot{\vec{\phi}}_e^T \{z^+\} \end{aligned} \tag{6}$$

where

$$[m^+] = [m] + [m_z] \tag{7}$$

$$[m] = \lambda \int_0^L \left( \vec{D}_y \vec{D}_y^T + \vec{D}_x \vec{D}_x^T \right) dx \tag{8}$$

$$[B] = 2\lambda \int_0^L \left( \vec{D}_y \vec{D}_x^T \right) dx \tag{9}$$

$$[m_z] = \frac{\lambda}{A} \int_0^L \left( \frac{\partial \vec{D}_y}{\partial x} \right) \left( \frac{\partial \vec{D}_y^T}{\partial x} \right) dx \tag{10}$$

$$\{y^+\} = \lambda \int_0^L \left( \dot{q}^2 x \vec{D}_x + V_{ay} \dot{q} \vec{D}_x - V_{ax} \dot{q} \vec{D}_y \right) dx \tag{11}$$

$$\{x^+\} = \lambda \int_0^L \left( \dot{q} y \vec{D}_y + V_{ay} \vec{D}_y + V_{ax} \vec{D}_x \right) dx \tag{12}$$

$$[z^+] = \frac{\lambda}{A} \int_0^L \left( \frac{\partial \vec{D}_y}{\partial x} \right) dx \tag{13}$$

The potential energy of an element is the sum of the strain energy and the energy due to gravity,

$$\begin{aligned} E_p = {} & \frac{1}{2} \int_0^L \left\{ EI \left( \frac{\partial^2 D_{ye}}{\partial x^2} \right)^2 + \frac{(EI)^2}{GA^*} \left( \frac{\partial^3 D_{ye}}{\partial x^3} \right)^2 \right. \\ & \left. + EA \left( \frac{\partial D_{xe}}{\partial x} \right)^2 \right\} dx + \lambda g \left\{ r_{ay} + \frac{1}{2} L \sin q_i \right. \\ & \left. + \int_0^L (D_{ye} \cos q_i + D_{xe} \sin q_i) \, dx \right\} \end{aligned} \tag{14}$$

where $r_{ay}$ is the geometric projection of $r_a$ (Fig. 3), $r_a$ is a vector extending from the global frame to the beam fixed frame, $E$ and $G$ represent the elastic and shear modulus, respectively, $A^*$ is the shear cross-sectional area, and $g$ is the gravitational acceleration vector. With substitution of Eqs. (2) and (3) into

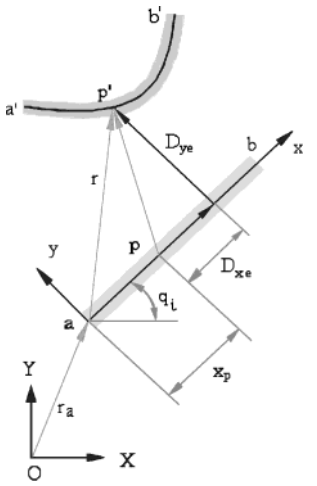


**Figure 3.** The deformation of a DLO element.

Eq. (14), then

$$E_p = \frac{1}{2}\vec{\phi}_e^T[K]\vec{\phi}_e + \lambda g\left\{r_{ay} + \frac{1}{2}L\sin q_i + \int_0^L \vec{\phi}_e^T\left(\vec{D}_y\cos q_i + \vec{D}_x \sin q_i\right) dx\right\} \quad (15)$$

The Lagrange equation for a DLO element is expressed as

$$\frac{d}{dt}\left(\frac{\partial E_k}{\partial \dot{\vec{\phi}}_e}\right) - \frac{\partial E_k}{\partial \vec{\phi}_e} + \frac{\partial E_p}{\partial \vec{\phi}_e} = \vec{q}_e + \vec{f} \quad (16)$$

Substituting Eqs. (6) and (15) into Eq. (16) and rearranging into a compact form gives

$$[m_e]\ddot{\vec{\phi}}_e + [c_e]\dot{\vec{\phi}}_e + [k_e]\vec{\phi}_e = \vec{p}_e + \vec{f}_e \quad (17)$$

where

$$[m_e] = [m] + [m_z] \quad (18)$$

$$[c_e] = 2\dot{q}[B] \quad (19)$$

$$[k_e] = \dot{q}[B] - \dot{q}^2[m] + [k] \quad (20)$$

$$\vec{p}_e = \vec{y}^+ - \vec{x}^+ - \vec{z}^+ - \vec{m}_g \quad (21)$$

$$\vec{m}_g = \lambda g\int_0^L \left(\vec{D}_y\cos q_i + \vec{D}_x\sin q_i\right) dx \quad (22)$$

and $\vec{f}_e$ is the external force given by the adjacent element.

It is evident that the damping matrix here is only determined by the symmetric mass matrix and the element's angular velocity. However, the damping effects vary for different DLOs; therefore the damping matrix of the element should be modified to deal with different DLOs. The following equations are introduced:

$$[c_e]' = [c_e] + [c]_m \quad (23)$$

where $[c]_m$ is the modifying matrix which can be obtained as

$$[c]_m = \xi[m_e]\begin{bmatrix} \ddots & & 0 \\ & \sqrt{k_{ii}/m_{ii}} & \\ 0 & & \ddots \end{bmatrix}_{8\times 8} \quad (24)$$

where $\xi$ is the damping coefficient, which can be determined by estimation or experiment, and $k_{ii}$ and $m_{ii}$ are the diagonal elements of $[k_e]$ and $[m_e]$, respectively. Based on Eqs. (23) and (24), we have modified the elemental dynamic equation

$$[m_e]\ddot{\vec{\phi}}_e + [c_e]'\dot{\vec{\phi}}_e + [k_e]\vec{\phi}_e = \vec{p}_e + \vec{f}_e \quad (25)$$

The elemental dynamic equations can be assembled into a dynamic system and expressed in terms of global variables:

$$[M]_s\{\ddot{\Phi}\} + [C]_s\{\dot{\Phi}\} + [K]_s\{\Phi\} = \{P\}_s \quad (26)$$

where $[M]_s$, $[C]_s$, and $[K]_s$ are, respectively, the mass, damping, and stiffness matrix of the system and $\{P\}_s$ is the load vector of the system.

The quasistatic equation, which only describes the stable deformations, can be obtained as

$$[K]_s\{\Phi\} = \{P\}_s \quad (27)$$

## 3. ADJUSTMENT-MOTION OF END-EFFECTOR

In a normal motion, DLOs go through an acceleration, constant velocity, and deceleration mode. Both acceleration and deceleration will cause vibration of DLOs. To avoid the vibration, a special trajectory can be designed. Most previous research involved attempts to damp the vibration during the complete trajectory.[19]

With regard to manipulation, only the vibration which could result in the failure of the next operation should be eliminated. Most important of all, the method used to eliminate vibration should be applicable in similar cases without necessitating major changes. Based on the above requirements, we present attachable adjustment-motions that can be conducted at the end of any arbitrary trajectory to damp the vibration caused by this previous motion. Adjustment-motion here refers to a kind of agile motion with limited scope.

### 3.1. Adjustment-Motion Classification

The attachable adjustment-motions can be divided into two different groups according to their motion styles. One is translation-adjustment-motion (TAMo) and another one is rotation-adjustment-motion (RAMo). The adjustment-motions can also be classified either as one-way adjustment-motion or two-way adjustment-motion. The different kinds of adjustment-motions presented in this article can be found in Table I.

### 3.2. One-Way Adjustment-Motion

A one-way RAMo is presented as an example to describe adjustment-motions in detail. As shown in Fig. 4, the adjustment-motion moves along a circle which assumes the nominal endpoint of the DLO as its center and the length of the DLO as its radius. The adjustment-motion starts from the last nominal position of the previous arbitrary trajectory and ends at a certain point of the circle.

**Table I.** Classification of adjustment-motions.

| | One-way | Two-way |
|---|---|---|
| TAMo | 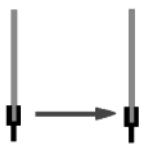 | 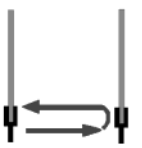 |
| RAMo |  |  |

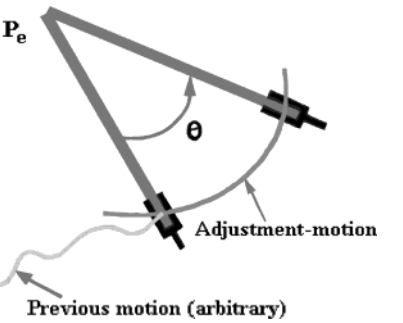


**Figure 4.** An one-way RAMo.

The profile of the one-way RAMo can be written as

$$x = L\cos\theta + x_{ed} \tag{28}$$

$$y = L\sin\theta + y_{ed} \tag{29}$$

where $x_{ed}$ and $y_{ed}$ describe the nominal position of the endpoint $p_e(x_{ed}, y_{ed})$ of the DLO. This point also acts as the center of the adjustment motion, and

$$\theta = \omega t \tag{30}$$

where $\omega$ is the constant angular velocity of the DLO during the adjustment.

By using this adjustment motion (Fig. 5), the DLO will be accelerated from rest to a velocity $\omega$. Then it is moved at this constant velocity for a certain period $t_a$. Deceleration is performed after this period to stop the adjustment motion.

There is a delay time between the previous arbitrary end-effector's trajectory and adjustment-motion, as shown in Fig. 5. The delay is useful in enabling the adjustment to take advantage of inertia. The optimal delay time can be determined by optimization methods. It should be noted that the

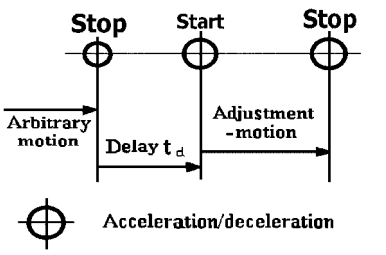


**Figure 5.** Scheme of an one-way RAMo.

constant velocity is the angular velocity for the DLO's circular motion.

For industrial robots, the time of acceleration and deceleration $\Delta t$ is quite small. It is reasonable to assume that the movement of the DLOs involves a sharp increase of the acceleration and deceleration (Fig. 6).

The relationships between acceleration (deceleration) and constant velocity are

$$\omega = \varepsilon_{acc} \Delta t_1 \tag{31}$$

and

$$\omega = -\varepsilon_{dec} \Delta t_2 \tag{32}$$

This implies that only two of the three parameters in Eqs. (31) or (32) must be determined. The parameters of adjustment-motion which should be determined by optimization are as follows: delay time $t_d$, value of acceleration (negative is also possible) $\varepsilon_{acc}$, the constant angular velocity $\omega$, the running time of this velocity $t_a$, and the value of deceleration $\varepsilon_{de}$.

The one-way TAMo can be defined in a similar way.

### 3.3. Two-Way Adjustment-Motion

When a robot manipulates a DLO, perhaps it is expected to return the DLO to its previous position as the final task to start the next operation. Two-way adjustment-motion is presented to meet this demand.

If a two-way adjustment-motion (either RAMo or TAMo) is conducted, the DLO will be handled and finally returned to the original position with the same posture after adjustment. A two-way adjustment-motion can be defined as two connected symmetrical parts as shown in Fig. 7, and each part is a one-way adjustment-motion. One may realize that a two-way adjustment-motion and a one-way adjustment-motion have the same number of parameters that should be determined by optimization methods. The details of a two-way adjustment-motion thus will not be described again.

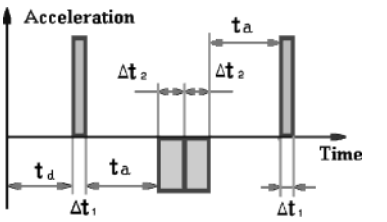


**Figure 7.** Acceleration profile of a two-way adjustment.

## 4. ADJUSTMENT-MOTION GENERATION BY GENETIC ALGORITHMS

As described in section 3, the adjustment-motion should be carefully selected to attain vibration reduction. Genetic algorithms (GAs) are evolutionary, stochastic and global search methods. Their performance is superior to those of classical techniques,[24,25] and they have been used successfully in robot path planning.[26,27] There has been little work reported involving application of this optimization method to trajectory generation for handling DLOs.

### 4.1. Objective and Constraint Functions

Since gravity is taken into account in this method, as stated above, the handling operation is not limited to the horizontal plane. The oscillation may not be symmetric with respect to its nominal position; therefore, the parameter which describes the amplitude of vibration is redefined here, as shown in Fig. 8.

The following objective function is minimized according to the defined parameter,

$$f = d_a \tag{33}$$

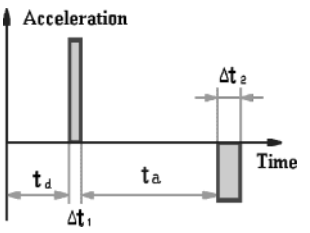


**Figure 6.** Acceleration profile of an one-way RAMo.

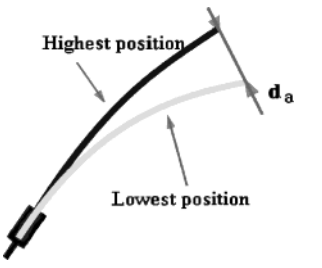


**Figure 8.** Vibrational amplitude of a DLO.

where $d_a$ is the maximum endpoint vibrational amplitude of a DLO as described in Fig. 8. Since the adjustment-motion cannot start before the delay time $t_d$, it is reasonable to account for the $d_a$ immediately after the delay period.

The adjustment motion planning problem for the vibration-free handling of DLOs can now be expressed as the following optimization problem:

$$\min: f = d_a \tag{34}$$

$$\text{s.t. } t_{d,\min} \le t_d \le t_{d,\max} \tag{35a}$$

$$\varepsilon_{ac,\min} \le \varepsilon_{ac} \le \varepsilon_{ac,\max} \tag{35b}$$

$$\omega_{\min} \le \omega \le \omega_{\max} \tag{35c}$$

$$t_{c,\min} \le t_c \le t_{c,\max} \tag{35d}$$

$$\varepsilon_{de,\min} \le \varepsilon_{de} \le \varepsilon_{de,\max} \tag{35e}$$

where $t_{d,\min}$ and $t_{d,\max}$ are the lower and upper permitted delay times, $\varepsilon_{\mathrm{ac},\min}$ and $\varepsilon_{ac,\max}$ are the lower and upper permitted DLO angular accelerations, $\omega_{\min}$ and $\omega_{\max}$ are the lower and upper permitted DLO constant angular velocities, $t_{c,\min}$ and $t_{c,\max}$ are the lower and upper permitted DLO constant angular velocities, and are the lower and upper permitted running times at the constant angular velocity along the adjustment circle, and $\varepsilon_{de,\min}$ and $\varepsilon_{de,\max}$ are the lower and upper DLO angular decelerations, respectively. The lower and upper limits of Eqs. (35b), (35c), and (35e) are determined by the capabilities of the robot. The maximum possible scope of adjustment-motions is determined mainly by the upper limits of Eq. (35d).

### 4.2. Optimization Method

As stated above, since the basic form of adjustment-motion is given, if the parameters of the adjustment-motion have been determined, then the attached adjustment can be easily determined. We use GAs to determine the adjustment-motion parameters. GA programs are described in detail in ref. 25. The GA procedure proposed to optimize adjustment-motion for handling of DLOs without serious residual vibration is shown in Fig. 9.

In the procedure, the coding method for the parameters is binary coding, which has been shown to be most effective for this type of parameter optimization.[25] The fitness function of the optimization is selected as being the maximum amplitude of deflection shortly after the delay period, which is the same as the objective function Eq. (34).

```
Procedure AMDLO
 BEGIN
    N:=0;
    Initialize ( P_N );
    Evaluate ( P_N );
    REPEAT
          Selection 2 parents from P_N ;
          Crossover ( P_N );
          Mutation ( P_N );
          Form new generation P_N ;
          Evaluate ( P_N );
          N:=N+1;
    UNTIL Termination Condition = True;
    Select adjustment-motion for DLO;
 END
```

**Figure 9.** Procedure to generate adjustment-motion for handling DLOs.

As shown in Fig. 9, initialization randomly generates an initial host population $P_0$. New generations are formed by survivors from the last generation and new individuals generated through mutation and crossover. Single-point crossover is used to form the new generation. The adjustment-motion is finally decided when the termination condition is satisfied. The termination condition of the procedure can be maximum generations or certain value according to next operation, such as the diameter of a hole through which the DLO is to be inserted.

## 5. CASE STUDIES

In these case studies, we use a long DLO described by two elements (Fig. 10). One of its ends, which is grasped by the end-effector, is treated as a cantilever without vibrational deflection to exclude curvature displacement. The other distal end is treated as a free end. Therefore, we use a total of eight general coordinates to describe the deformed shape of the DLO.

The cross section of the DLO is rectangular. All of the cases are situated in the vertical plane. The gravitational acceleration is 9.80 m/s$^2$. The physical parameters of the DLO are given in Table II.

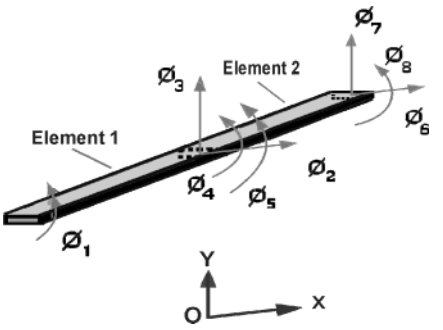


**Figure 10.** General coordinates of a DLO.

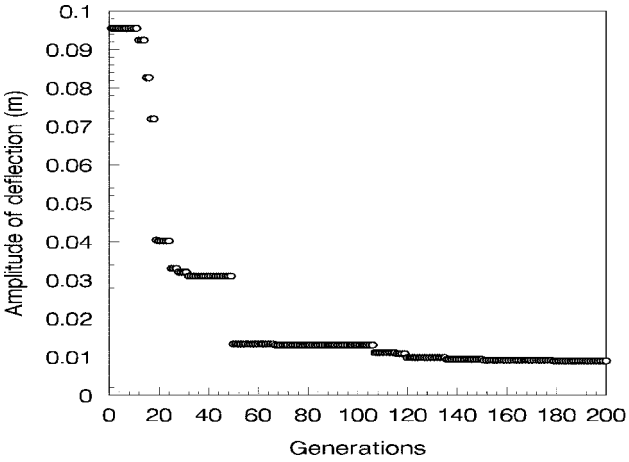


**Figure 11.** Amplitude of deflection of the DLO versus number of generations (previous motion: rotation).

### 5.1. Cases of One-Way RAMo

The following three cases are simulated using a one-way RAMo as the adjustment type. The previous motions of the cases are rotation, translation, and combined rotation and translation, respectively.

#### 5.1.1. Case One

Suppose that the previous end-effector's motion is rotational. The adjustment-motion begins after the rotation and a certain delay. The process of generating the parameters takes about 30 minutes using a Pentium 500 MHz computer. In this case, the GA-generated parameters are delay time 0.047 s, value of acceleration $-59.530$ rad/s$^2$, constant angular velocity $-2.401$ rad/s, running time at this velocity 0.131 s, and value of deceleration 50.054 rad/s$^2$. The results are given in the following figures.

Figure 11 shows the vibrational amplitude versus the number of completed GA generations. The shape, vibration, and motion of the DLO with and without adjustment-motion are shown and compared in Fig. 12. The vibrational and adjustment-motion portions of the complete motion are both shown again separately in the lower portion of the figure. A detailed comparison of the vibrational amplitudes resulting from these two situations is shown in Fig. 13. It was found that the adjustment-motion can effectively reduce the vibrational amplitude.

**Table II.** Parameters of the DLO.

| | |
|---|---|
| Length of DLO | 1.0 m |
| Length of element | 0.5 m |
| Width of DLO | 11 mm |
| Height of DLO | 0.5 mm |
| Elastic modules | $1.26 \times 10^{11}$ Pa |
| Shear modules | $0.70 \times 10^{11}$ Pa |
| Density | 8960 kg/m$^3$ |
| Damping coefficient | 0.0005 |

#### 5.1.2. Case Two

Suppose the previous end-effector's motion is translation. The adjustment-motion begins after the translation and a certain delay. In this case, the GA-generated parameters are delay time 0.068 s, value of acceleration $-96.481$ rad/s$^2$, constant angular velocity $-3.001$ rad/s, running time at this velocity 0.117 s, and value of deceleration 56.798 rad/s$^2$. The results are found in the following figures.

Figure 14 shows the vibrational amplitude versus number of completed GA generations. The shapes and motions of the DLO with and without an adjustment-motion are shown and compared in Fig. 15. A detailed comparison of the vibrational amplitude resulting from these two situations is shown in Fig. 16. It was again found that the adjustment-motion can effectively reduce the vibrational amplitude.

#### 5.1.3. Case Three

To verify the effectiveness of this method based on a more general previous motion, we present here another case study. In this example, the initial motion combines rotation and translation. In case three, the GA-generated parameters are delay time 0.200 s, value of acceleration $-97.263$ rad/s$^2$, constant

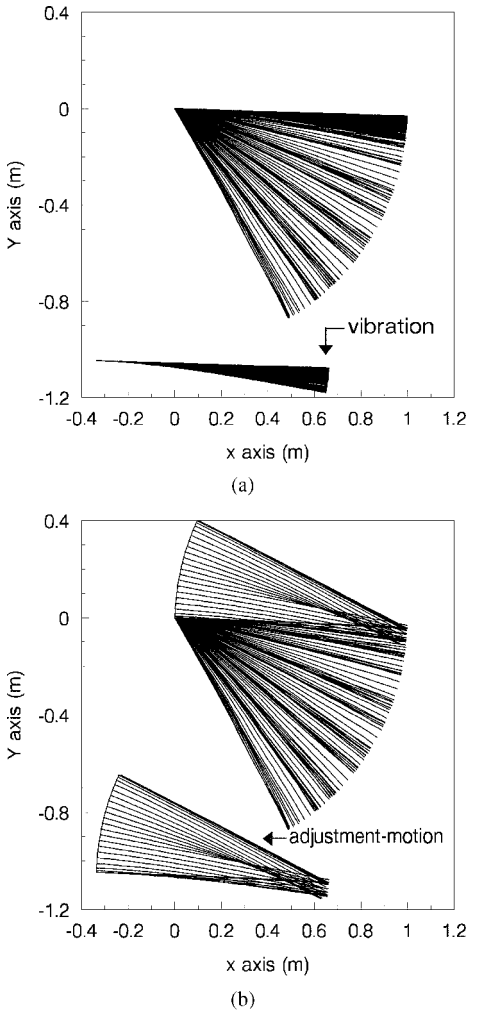


**Figure 12.** The previous motion, vibration, and one-way RAMo of the DLO. (a) End-effector stops after the rotation. (b) End-effector adjusts after the rotation.

angular velocity $-4.000$ rad/s, running time at this velocity 0.164 s, and value of deceleration 57.971 rad/s$^2$.

The results are shown in Figs. 17–19. It was found once again that the attached adjustment-motion is effective in reducing vibrations of the DLO. This implies that the adjustment-motion skill can be attached to any complex previous motions.

### 5.2. Cases with Different Adjustment-Motion Styles

The above cases show the effectiveness of one-way RAMos. How about the other adjustment-motion styles? In the following cases, different styles are used to reduce vibration caused by the same previous motion. A combined rotation and translation is used as the previous motion.

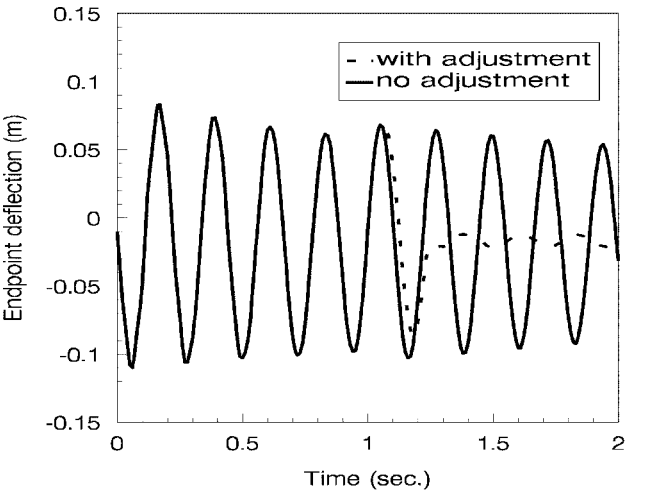


**Figure 13.** Deflection of the DLO with and without one-way RAMo. (previous motion: rotation).

#### 5.2.1. One-Way TAMo

In this case, TAMo is chosen as the adjustment style. The GA-generated parameters are delay time 0.125 s, value of acceleration $-39.198$ m/s$^2$, constant velocity $-2.023$ m/s, running time at this velocity 0.055 s, and value of deceleration 52.551 m/s$^2$. The results are shown in Figs. 20–22. It was found that the method using a TAMo is quite effective.

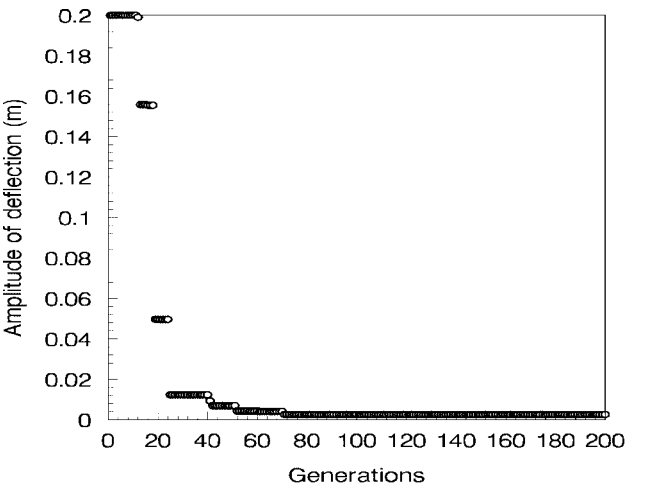


**Figure 14.** Amplitude of deflection of the DLO versus number of generations (previous motion: translation).

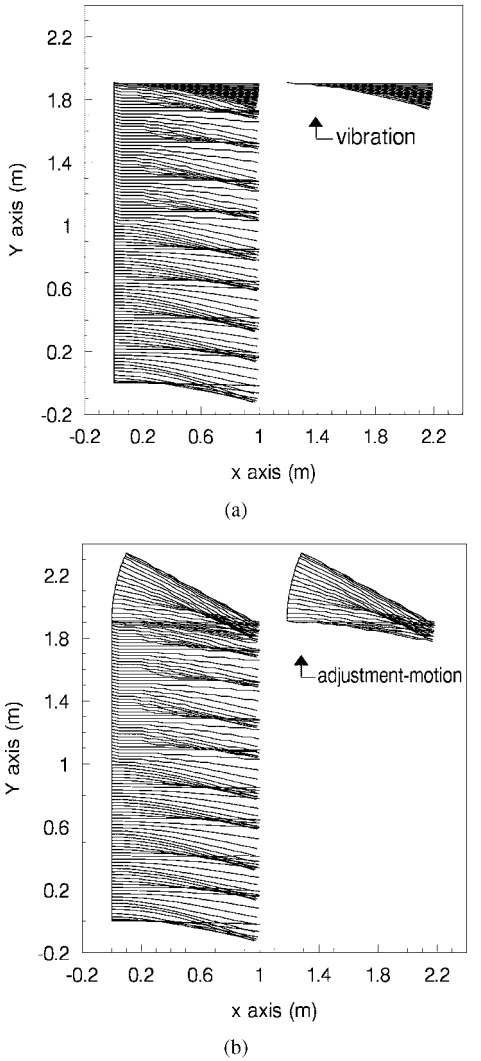


**Figure 15.** The previous motion, vibration, and one-way RAMo of the DLO. (a) End-effector stops after the translation. (b) End-effector adjusts after the translation.

### 5.2.2. Two-Way RAMo

In this two-way case study, RAMo is chosen as the adjustment style. The GA-generated parameters are delay time 0.342 s, value of acceleration 61.486 rad/$s^2$, constant angular velocity 3.867 rad/s, running time at this velocity 0.012 s, and the value of deceleration $-91.829$ rad/$s^2$. The results are given in Figs. 23–25, respectively. It was found that the two-way RAMo is also effective.

### 5.2.3. Two-Way TAMo

In this two-way case study, TAMo is chosen as the adjustment style. The GA-generated parameters are delay time 0.248 s, value of acceleration 74.585 m/$s^2$,

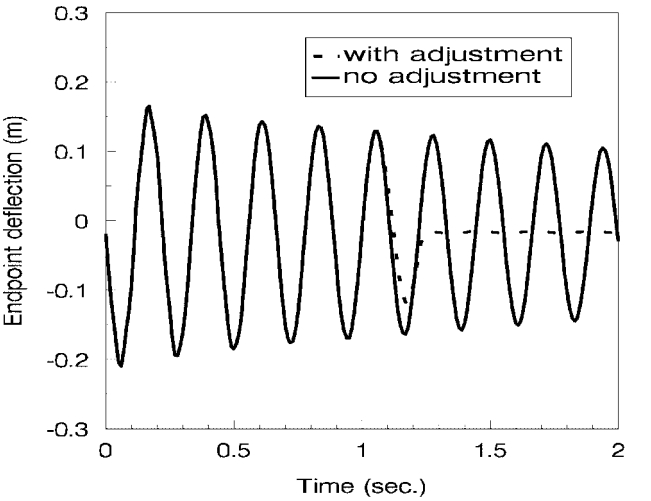


**Figure 16.** Deflections of the DLO with and without one-way RAMo. (previous motion: translation).

constant velocity 1.114 m/s, running time at this velocity 0.095 s, and the value of deceleration $-41.409$ m/$s^2$. The results are given in the Figs. 26–28. It was found that the two-way TAMo is quite effective in reducing vibration resulted from previous motion.

The above cases proved that for the same previous motion, each style can decrease vibration amplitude efficiently with slight differences in the results. Which one to use in practice is probably decided by the environment in which the method is to be applied.

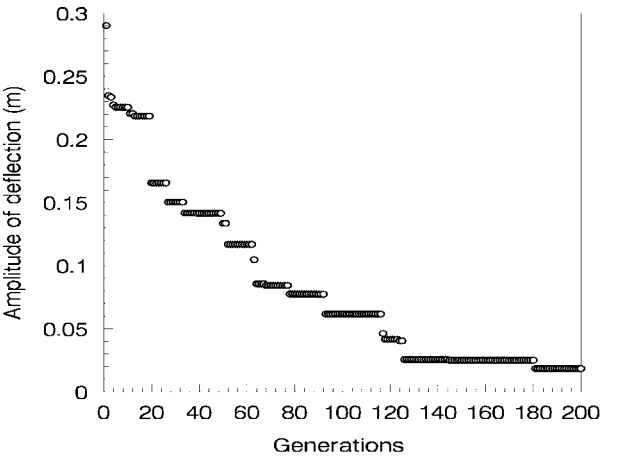


**Figure 17.** Amplitude of deflection of the DLO versus number of generations (previous motion: combined rotation and translation).

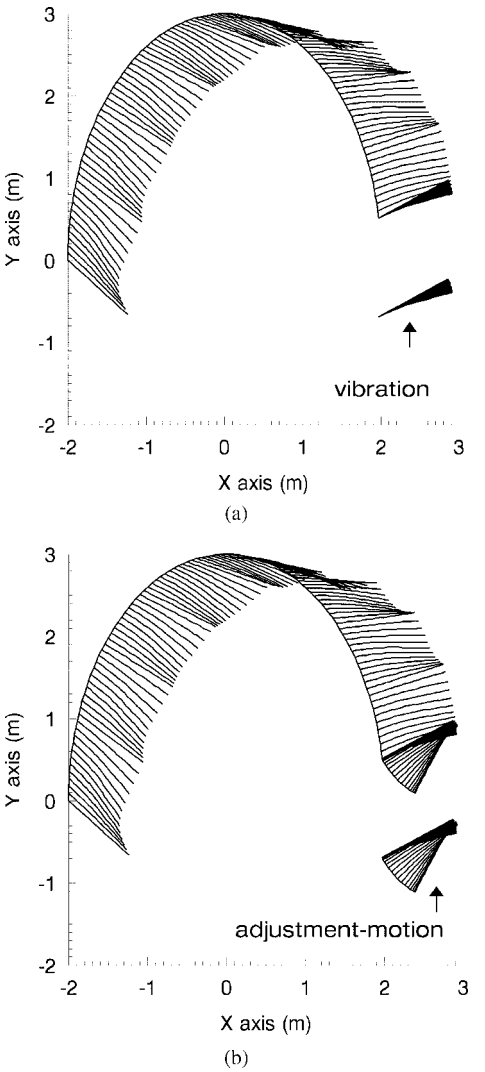


**Figure 18.** The previous motion, vibration, and one-way RAMo of the DLO. (a) End-effector stops after initial motion. (b) End-effector adjusts after initial motion.

## 6. EXPERIMENT

To verify the method presented and simulated above, an experiment was conducted using a Stäubli RX130 industrial robot (Fig. 29). A standard 500-mm stainless ruler is used as the DLO in the experiment. Considering that one end of the ruler is grasped by the jaws, the actual length of the ruler is 490 mm. The cross section of the ruler is $0.5 \times 18$ mm. A density of 7880 kg/m$^3$ and an elastic modulus of $368 \times 10^6$ N/m$^2$ are used in the simulation. The previous motion is assumed to be a translation of 600 mm within 1 s and the adjustment-motion style is one-way TAMo. The experiment is conducted in the horizontal plane.

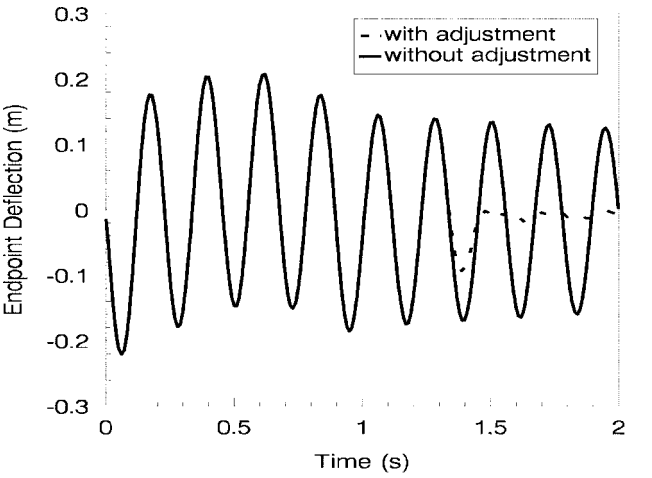


**Figure 19.** Deflections of the DLO with and without adjustment-motion (previous motion: combined rotation and translation).

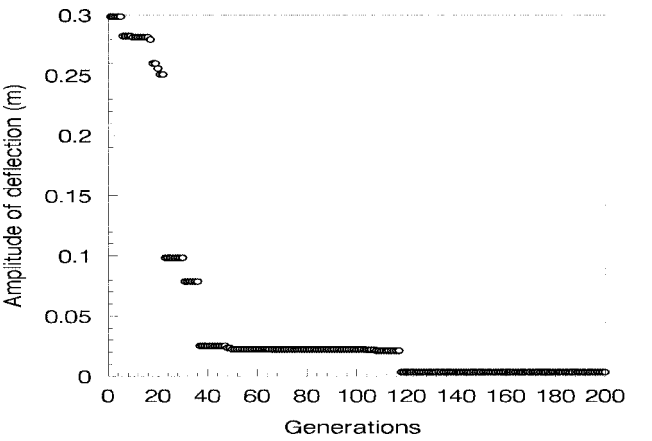


**Figure 20.** Amplitude of deflection of the DLO versus number of generations by using one-way TAMo.

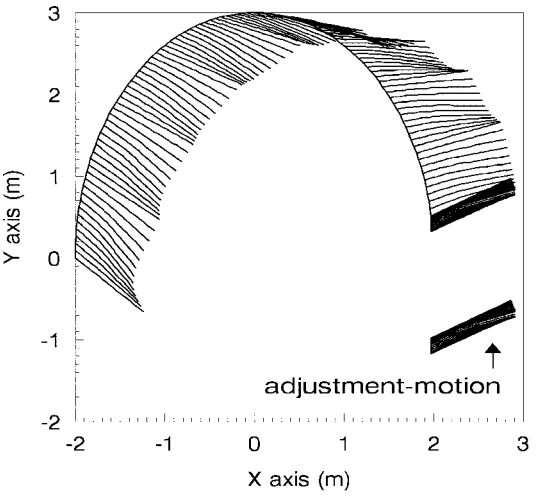


**Figure 21.** The previous motion and one-way TAMo of the DLO.

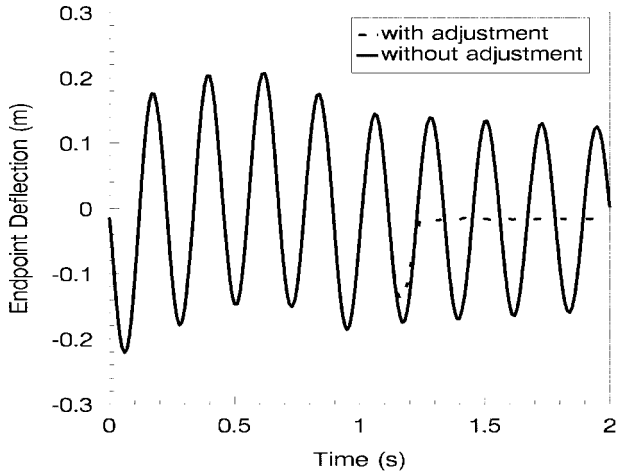


**Figure 22.** Deflection of the DLO with and without one-way TAMo.

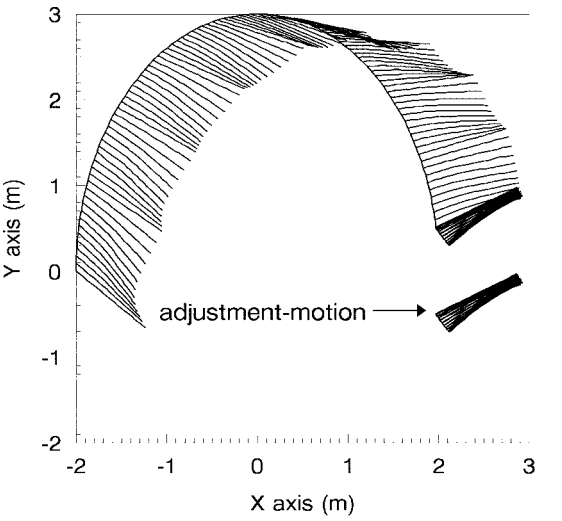


**Figure 24.** The previous motion and two-way RAMo of the DLO.

First, the adjustment-motion is generated by simulation. After 60 generations, the simulation results are obtained. The GA-generated parameters are: 0.357 s delay time, 8.867 $m/s^2$ acceleration, 0.724 m/s velocity, 0.046 s running time at this velocity, and $-8.517$ $m/s^2$ deceleration. Then, these parameters are downloaded to the RX130 control unit with real-time V+ language. The maximum vibrational amplitude obtained by simulation, experiment, and hand improvement are compared in Fig. 30.

All of the vibrational amplitudes are decreased sharply by the adjustment-motions. However, with the same adjustment, the amplitude of the experimental results is almost two times larger than that of the simulation results. This probably happens for two reasons: model errors and robot-limited resolution. Model errors include the error resulting from the method and the error caused by parameter measuring of the DLO. Figure 30 also indicates this aspect, showing a comparison of vibrational amplitudes without adjustment. As to the second source of error, every robot has its limited capabilities when operating under definite demands. Therefore, hand-improved results are also shown in Fig. 30. The hand-improved results are obtained by extending the delay time to 0.4 s, the constant velocity to 0.750 m/s, and both acceleration and deceleration to 9.000 $m/s^2$.

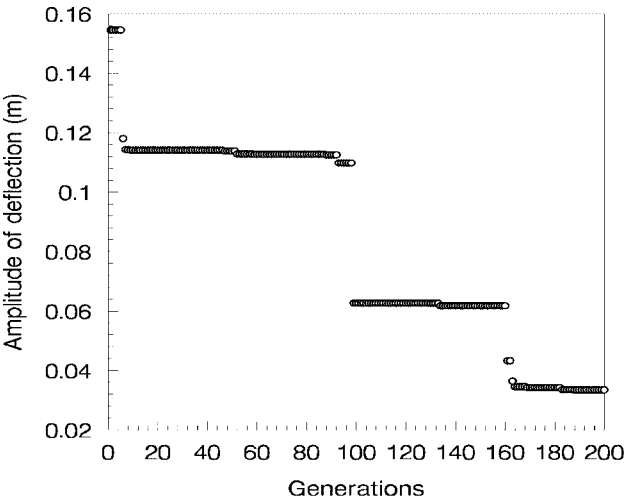


**Figure 23.** Amplitude of deflection of the DLO versus number of generations by using two-way RAMo.

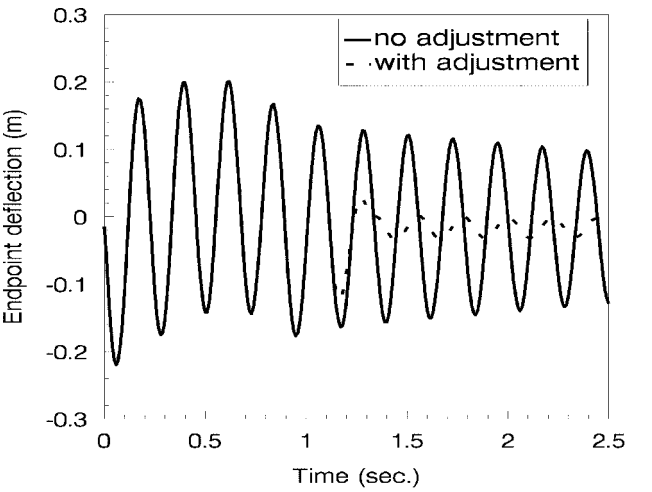


**Figure 25.** Deflection of the DLO with and without two-way RAMo.

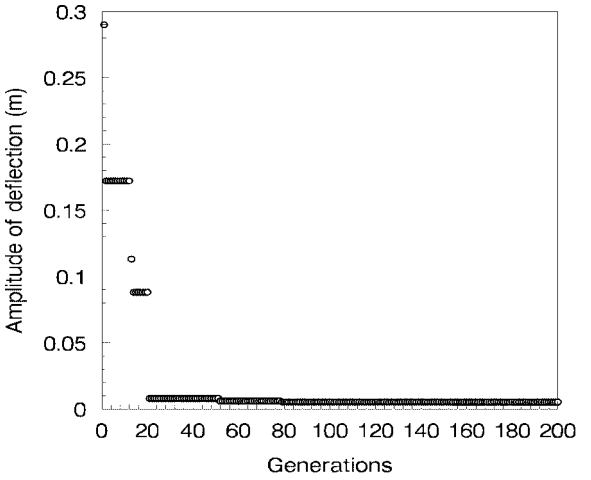


**Figure 26.** Amplitude of deflection of the DLO versus number of generations by using two-way TAMo.

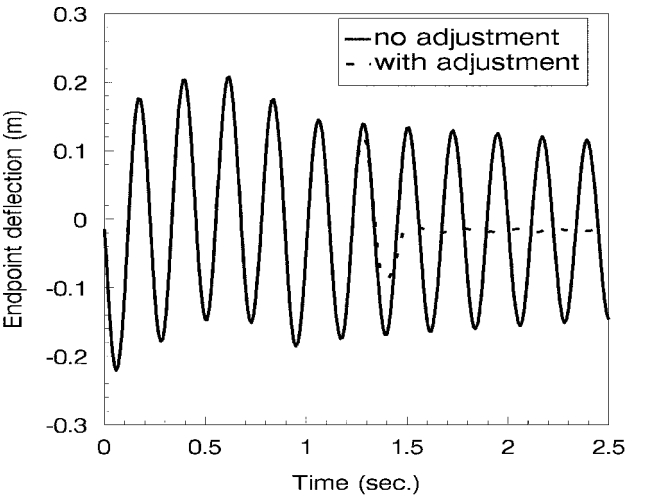


**Figure 28.** Deflection of the DLO with and without two-way TAMo.

Since the slight changes around the GA-generated parameters did not result in sharp changes of the vibrational amplitude of the DLO, the hand-improved results also show the robustness of the attachable adjustment-motion.

Based on the results and discussion of the experiment, the presented method has been proved to be applicable in practice.

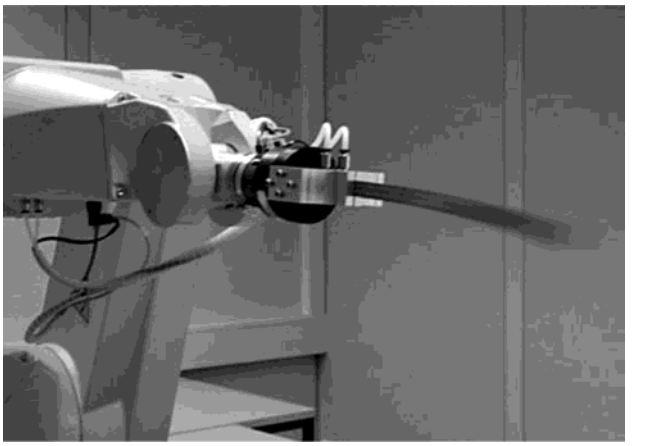

**Figure 29.** One-way TAMo of the DLO by the end-effector of a RX130 robot.

## 7. CONCLUSION

In this article, we have addressed the problem of manipulating deformable linear objects in a way suitable to avoid acute vibration. Different kinds of

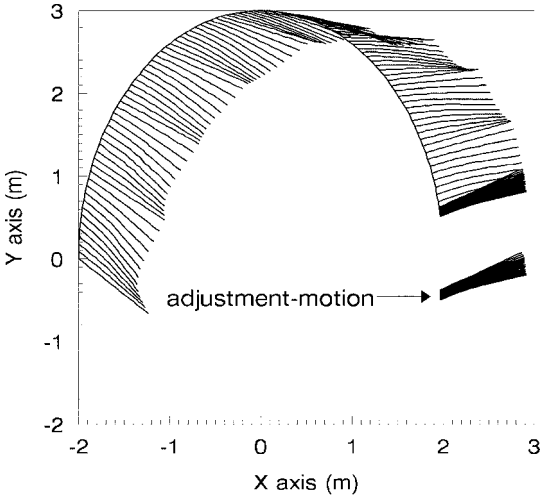


**Figure 27.** The previous motion and two-way TAMo of the DLO.

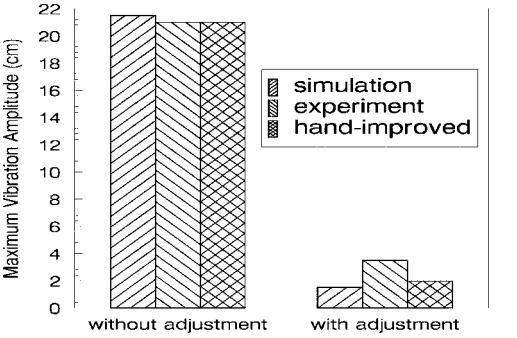


**Figure 30.** Comparison of results from simulation and experiment.

adjustment-motions have been presented, which can be attached to the end of any arbitrary end-effector's trajectory to eliminate unwanted vibration of the object. For describing the dynamics of deformable linear objects, a finite element method was used to derive the dynamic differential equations. A genetic algorithm was applied to find the optimal adjustment-motion for each simulation example. The case studies showed that adjustment-motion is suitable for eliminating vibration arising during handling of deformable linear objects. An experiment was also conducted and verified the presented method.

Detailed information about previous motions is necessary since sensors are not used in the open-loop method presented. In the future, a new sensor-based method which can use sensors to determine the adjustment-motion will be presented. The sensor-based method can be attached and computed on-line instead of off-line. The information about the previous motion will not be necessary if the sensor-based method is used.

## APPENDIX

$$\vec{D}_x = \begin{bmatrix} 1 - \frac{1}{L}x \\ 0 \\ 0 \\ 0 \\ \frac{1}{L}x \\ 0 \\ 0 \\ 0 \end{bmatrix}_{8\times 1}$$

$$\vec{D}_y = \begin{bmatrix} 0 \\ 1 - \frac{10}{L^3}x^3 + \frac{15}{L^4}x^4 - \frac{6}{L^5}x^5 \\ x - \frac{6}{L^2}x^3 + \frac{8}{L^3}x^4 - \frac{3}{L^4}x^5 \\ \frac{1}{2}x^2 - \frac{3}{2L}x^3 + \frac{3}{2L^2}x^4 - \frac{1}{2L^3}x^5 \\ 0 \\ \frac{10}{L^3}x^3 - \frac{15}{L^4}x^4 + \frac{6}{L^5}x^5 \\ -\frac{4}{L^3}x^3 + \frac{7}{L^4}x^4 - \frac{3}{L^5}x^5 \\ \frac{1}{2L}x^3 - \frac{1}{L^2}x^4 + \frac{1}{2L^3}x^5 \end{bmatrix}_{8\times 1}$$

The support of the Alexander von Humboldt Foundation is greatly appreciated by the first author. We thank Mr. Dirk Ebert and Mr. Thorsten Schmidt for their kind help in preparing pictures.

## REFERENCES

1. A. Villarreal and H. Asada, A geometric representation of distributed compliance for the assembly of flexible parts, Proc IEEE Int Conf Robotics Automat, 1991, pp. 2708–2715.
2. H. Nakagaki, K. Kitagaki, T. Ogasawara, and H. Tsukune, Study of insertion task of a flexible beam into a hole by using visual tracking observed by stereo vision, Proc IEEE Int Conf Robotics Automat, Minneapolis, 1996, vol. 4, pp. 3209–3214.
3. H. Nakagaki, K. Kitagaki, T. Ogasawara, and H. Tsukune, Study of deformation and insertion task of a flexible wire, Proc IEEE Int Conf Robotics Automat (ICRA'97), Albuquerque, 1997, vol. 3, pp. 2397–2402.
4. H. Wakamatsu, T. Matsumura, E. Arai, and S. Hirai, Dynamic analysis of rod like object deformation towards their dynamic manipulation, Proc IEEE/IROS Int Conf Intell Robots Syst, 1997, pp. 196–201.
5. H. Wakamatsu, S. Hirai, and K. Iwata, Static analysis of deformable object grasping based on bounded force closure, Proc IEEE Int Conf Robotics Automat, Minneapolis, 1996, vol. 4, pp. 3324–3329.
6. K. Higashijima, H. Onda, and T. Ogasawara, Planning for wire obstacles avoidance using ultrasonic sensors, 8th Int Conf Advance Robotics (ICRA'97), California, 1997, pp. 577–582.
7. P.W. Smith, N. Nandhakumar, and A.K. Tamadorai, Vision based manipulation of non rigid objects, Proc IEEE Int Conf Robotics Automat, Minneapolis, 1996, vol. 4, pp. 3191–3196.
8. S. Hirai, H. Wakamatsu, and K. Iwata, Modeling of deformable thin parts for their manipulation, Proc IEEE Int Conf Robotics Automat, San Diego, 1994, vol. 4, pp. 2955–2960.
9. S. Hirai, H. Noguchi, and K. Iwata, Transplantation of human skillful motion to manipulators in insertion of deformable tubes, Proc IEEE Int Conf Robotics Automat, Nagoya, 1995, vol. 2, pp. 1900–1905.
10. S. Hirai and H. Wakamatsu, Modeling of deformable strings with bend, twist, and extension in 3D space, Proc 2nd ECPD Int Conf Advanced Robotics, Intell Automat Active Syst, Vienna, 1996, pp. 529–534.
11. S. Hirai, H. Noguchi, and K. Iwata, Human-demonstration based approach to the recognition of process state transitions in insertion of deformable tubes, Proc IEEE Int Conf Robotics Automat, Minneapolis, 1996, vol. 3, pp. 2006–2011.
12. T. Yukawa, M. Uchiyama, D.N. Nenchev, and H. Inooka, Stability of control system in handling of a flexible object by rigid arm robots, Proc IEEE Int Conf Robotics Automat, Minneapolis, 1996, pp. 2332–2338.
13. Y.F. Zheng, R. Pei, and C. Chen, Strategies for automatic assembly of deformable objects, Proc IEEE Int Conf Robotics Automat, 1991, pp. 2598–2603.
14. T. Hasegawa, T. Suehiro, and T. Takase, A model-based manipulation system with skill-based execution, IEEE Trans Robotics Automat, 8 (1992), 535–544.

15. H. Onda, H. Hirukawa, and K. Takase, Assembly motion teaching system using position/force simulator—extracting a sequence of contact state transition, Proc IEEE/RSJ Int Conf Intell Robots Syst, 1995, vol. 1, pp. 9–16.
16. D. Henrich, T. Ogasawara, and H. Wörn, Manipulating deformable linear objects—contact states and point contacts, IEEE Int Symp Assembly and Task Planning (ISATP'99), Porto, Portugal, 1999.
17. F. Abegg, A. Remde, and D. Henrich, ''Force and vision based detection of contact state transitions,'' Robot manipulation of deformable objects, D. Henrich and H. Wörn (Editors), Springer-Verlag, London, 2000.
18. A. Remde, D. Henrich, and H. Wörn, Picking-up deformable linear objects with industrial robots, Int Symp Robotics (30th ISR), Tokyo, 1999.
19. M.Z. Chen, and Y.F. Zheng, Vibration-free handling of deformable beams by robot end-effectors, J Robotic Syst 12 (1995), 331–347.
20. J.F. Jones and B.J. Petterson, Oscillation damped movement of suspended objects, Proc IEEE Int Conf Robotics Automat, 1988, pp. 956–962.
21. G.P. Starr, Swing-free transport of suspended objects with a path-controlled robot manipulator, J Dyn Syst Cont Trans ASME, (1985), 97–100.
22. W.L. Cleghorn, R.G. Fenton, and B. Tabarrok, Finite element analysis of high-speed flexible mechanisms, Mech Mach Theor, 16 (1981), 407–424.
23. S.G. Yue, Y.Q. Yu, and S.X. Bai, Flexible rotor beam element for manipulators with joint and link flexibility, Mech Mach Theor 32 (1997), 209–219.
24. D.B. Fogel, An introduction to simulated evolutionary optimization, IEEE Trans Neural Networks 5 (1994), 3–14.
25. D.E. Goldenberg, Genetic algorithms in search, optimization and machine learning, Addison-Wesley, Reading, MA, 1989.
26. N. Kubota, T. Arakawa, T. Fukuda, and K. Shimojima, Trajectory generation for redundant manipulator using virus evolutionary genetic algorithm, Proc IEEE Int Conf Robotics Automat, 1997, pp. 205–210.
27. S.D. Sun, A.S. Morris, and A.M.S. Zalzala, Trajectory planning of multiple coordinating robots using genetic algorithms, Robotica 14 (1996), 227–234.